

Non-orthogonal Age-Optimal Information Dissemination in Vehicular Networks: A Meta Multi-Objective Reinforcement Learning Approach

Ahmed A. Al-Habob, *Member, IEEE*, Hina Tabassum, *Senior Member, IEEE*, and Omer Waqar, *Senior Member, IEEE*

Abstract—This paper considers minimizing the age-of-information (AoI) and transmit power consumption in a vehicular network, where a roadside unit (RSU) provides timely updates about a set of physical processes to vehicles. We consider non-orthogonal multi-modal information dissemination, which is based on superposed message transmission from RSU and successive interference cancellation (SIC) at vehicles. The formulated problem is a multi-objective mixed-integer nonlinear programming problem; thus, a Pareto-optimal front is very challenging to obtain. First, we leverage the weighted-sum approach to decompose the multi-objective problem into a set of multiple single-objective sub-problems corresponding to each predefined objective preference weight. Then, we develop a hybrid deep Q-network (DQN)-deep deterministic policy gradient (DDPG) model to solve each optimization sub-problem respective to predefined objective-preference weight. The DQN optimizes the decoding order, while the DDPG solves the continuous power allocation. The model needs to be retrained for each sub-problem. We then present a two-stage meta-multi-objective reinforcement learning solution to estimate the Pareto front with a few fine-tuning update steps without retraining the model for each sub-problem. Simulation results illustrate the efficacy of the proposed solutions compared to the existing benchmarks and that the meta-multi-objective reinforcement learning model estimates a high-quality Pareto frontier with reduced training time.

Index Terms—Age-of-information (AoI), deep reinforcement learning (DRL), meta deep reinforcement learning (meta-DRL), multi-objective optimization, successive interference cancellation (SIC).



1 INTRODUCTION

VEHICULAR communication networks enable a wide range of applications which require real-time updates, such as highly prioritized road safety applications (such as collision warning and adaptive cruise control) and the infotainment services such as news, media and social entertainments, which require real-time updates [1]. With the increasing diversity of vehicular applications that require real-time information updates, such as blind spot/lane change and forward collision warnings, communications in vehicular networks become time-critical, and thus, fresh status updates are of high importance [2].

Although the conventional communication latency and throughput are effective metrics to evaluate the performance of the vehicular communication networks, these metrics do not capture the information freshness which is critical to obtain the real-time knowledge about the location, orientation, and speed of the vehicles. To this end, the age-of-

information (AoI) is a useful metric to quantify the freshness of the information while taking into account the transmission latency, update generation time, and inter-update time interval. Specifically, AoI is defined as the elapsed time between the received information at the destination and the time when it was generated at the source [3]. It should be noted that the inter-update time—which is a scheduling parameter—is a crucial parameter in the AoI [3], and thus optimizing AoI is totally different from optimizing other metrics such as the throughput and latency.

Along another note, the existing state-of-the-art considers minimizing the AoI in uni-modal information dissemination scenario, where the destination/vehicle receives updates about a single application or physical process. However, a more practical scenario that should be addressed is the multi-modal information dissemination, in which each vehicle is interested in maintaining fresh status updates for one or more applications (physical processes). The straightforward strategy is to broadcast updates about all physical processes to all vehicles at each time slot. However, such a strategy consumes the transmitter’s power. Consequently, the trade-off between maintaining information freshness and reserving the power consumption should be handled to satisfy the decision-maker’s preference. Such a trade-off mandates a proper multi-objective optimization framework that handles the decision-maker’s preference by considering efficient messages’ encoding scheme to unicast/multicast updates and allocating the power in vehicular networks.

This work was supported by two Discovery Grants funded by the Natural Sciences and Engineering Research Council of Canada (NSERC).

At the time of this work, A. A. Habob was with the Department of Electrical Engineering and Computer Science at York University, Toronto, Canada. He is currently with the Memorial University of Newfoundland, Canada.

H. Tabassum is with the Department of Electrical Engineering and Computer Science, York University, Toronto, ON, Canada.

O. Waqar is with the School of Computing, University of the Fraser Valley, BC, Canada and also affiliated as an adjunct faculty member with the Department of Electrical Engineering and Computer Science, York University, Toronto, ON, Canada.

E-mails: alhabob@mun.ca, hinat@yorku.ca, Omer.Waqar@ufu.ca.

Traditionally, optimization approaches tackle the resource allocation in vehicular networks [4]. However, the communication channels in vehicular networks are rapidly varying. Furthermore, optimizing time-dependent metrics such as AoI involves a sequential decision-making over time. Thus, iterative and computationally complex optimization approaches are not well-suited. To this end, deep reinforcement learning (DRL) has been considered as a promising solution to learn a better policy on decision-making problems that are evolving over time [5], [6].

DRL paradigm has witnessed dramatic evolution to handle complex scenarios such as discrete-continuous hybrid action space and different training and testing environments [7]. A variant of the DRL is the multi-objective reinforcement learning (MORL) [8], in which the agent aims at optimizing multiple conflicting objectives. MORL inherits the well-known challenges of multi-objective optimization¹, including the trade-off between objectives with different units, ranges, and order of magnitude [12].

To address the aforementioned issues, a DRL agent can be trained and tested to find the preferred Pareto optimal solution based on the decision-maker's preference. The drawback is that the DRL agent needs to be retrained if the objectives' preference is modified or the vehicular communication environment is changed. Recently, meta-DRL concept has been introduced to enable the agent to quickly adapt to new environments by learning the agent a meta-policy that solves multiple tasks from a given distribution [14]. Meta-learning (or the learning to learn) can leverage knowledge from previous experiences to rapidly adapt to new/unseen tasks with few training (fine-tuning) steps [14], [15]. In this context, meta-DRL can be considered a posteriori paradigm to address the objectives' preference issue, in which the meta-DRL is trained to find the Pareto optimal solutions of a set of objectives' preferences which can be adapted or fine-tuned to the desirable solution [15], [16].

1.1 Related Works

Optimizing AoI in vehicular networks has been investigated in different scenarios [2], [5], [17], [18], [19]. In [17], a greedy algorithm was developed to minimize the expected sum AoI in a vehicular beacon broadcasting system and mitigate beacons' signals collision. In [18], a Lyapunov optimization solution was developed to minimize the transmit power in a vehicle-to-vehicle (V2V) network to facilitate ultra-reliable low-latency V2V communications subject to probabilistic AoI constraints. A proactive DRL technique was proposed in [5] to provide an AoI-aware radio resource management in vehicular networks with Manhattan grid road topology. In [19], the impact of inter-update generation, selection of fog/cloud servers, and processing delay on the AoI was studied in a vehicular shuttle system. A deep Q-learning algorithm was developed to optimize the vehicles' routing to improve the average AoI. In [2], the social relations among users in the vehicle network were considered in an AoI-centric information dissemination model. The authors

considered joint optimization of the information update rate and the transmit probabilities to minimize AoI.

Different unicast-multicast scenarios were considered in literature to transmit multiple messages to a group of users [20], [21], [22], [23], [24]. In [20], a non-orthogonal multiple access (NOMA) unicast-multicast scenario was designed, in which a set of unicast users (each requires unique message) and a set of multicast users (those who require an identical message) shares the same time/space/frequency resource. In this scenario, the messages of unicast users were encoded according to their channels' quality and the multicast message was superposed as the last encoded message. An integrated multicast-unicast scenario was proposed in [21], [22], such that each user receives a private message and a common message was broadcasted to all users. Sum-rate maximization was considered in [21], while the authors of [22] considered maximizing the energy efficiency in a simultaneous wireless information and power transfer protocol. In [23], a joint unicast and multi-group multicast transmission has been considered, in which a user is either a unicast or belongs to a group of multicast users. In [24], a fixed interval transmission strategy was considered to minimize the average AoI in a unilateral multicast network. The considered network consists of a base-station (BS) broadcasting time-sensitive updates to a set of users, in which the BS decides to broadcast an update packet at time. In [25], a digital twin-driven vehicular task offloading was studied to provide augmented computing capacities for internet of vehicles (IoV) scenario by considering mobile edge computing (MEC) and intelligent reflective surface (IRS). To reduce the overall delay and energy consumption, a two-stage optimization approach was developed for Jointly Optimizing Task Offloading and IRS Configuration. Another IoV scenario was studied in [26], in which an asynchronous federated broad learning (FBL) framework integrates broad learning (BL) into federated learning (FL).

Studying AoI in unicasts/multicasts scenarios has been considered in literature [27], [28], [29], [30], [31]. In [27], the average and peak AoI of multicast transmission with deadlines has been considered. An access point transmits timestamped status updates to multiple devices and the status update is terminated if either a subset of devices devices successfully receive the status update or the deadline expires. In [28], a multicast scheduling strategy has been proposed to improve the energy efficiency and AoI. The server transmits information to multiple users by queuing and bundling the requests from different users and serving users requesting the same contents. In [29], the AoI in multicast networks with retransmissions has been studied, in which the updates are encoded as a short blocklength packets and is broadcasted to multiple destinations via independent and identically distributed error-prone channels. The stopping threshold, the average AoI and EE expressions for stopping and wait-for-all schemes are derived as a function of the packet length. In [30], an architecture of AoI in multicast/unicast/device-to-device (D2D) transmission with a cell-free massive multiple-input multiple-output (MIMO) was studied. An age-optimum unicast-multicast scheduling of multiple update messages to vehicles has been considered in [31]. In this framework, at most an update about one physical process is scheduled to a vehicle at each

1. The conventional strategy to handle multi-objective optimization is to convert the problem into a single objective optimization problem, which can be implemented using ϵ -constraint approach [9], Tchebycheff approach [10], or weighted sum approach [11], [12], [13].

time slot. Ant colony optimization algorithm and deep Q-learning model were developed to solve a weighted sum optimization problem of the AoI and power consumption.

1.2 Motivation and Contributions

None of the research works to date considered the *non-orthogonal multi-modal information dissemination* in a vehicular network with *multiple conflicting objectives such as AoI minimization and power consumption minimization simultaneously*. We cast this problem as a multi-objective optimization problem (MOOP) and demonstrate the efficacy and the generalization capability of the *meta multi-objective RL* for estimating the **Pareto front** of the MOOP. Estimating the Pareto front in MOOP is essential, as it enables the decision-maker to optimize the conflicting objectives without the need to pre-determine the preference weight corresponding to each Pareto point. It is shown that the proposed model can estimate the entire Pareto front using few fine-tuning update steps, without the need to retrain a new DRL model for each point in the Pareto front. To summarize the existing work and highlight our key contributions, Table 1 summarizes the related work in terms of considering key techniques such as minimizing AoI, meta-DRL, meta-MORL, etc. The main contributions of this paper can then be summarized as follows:

- This paper proposes a *non-orthogonal* multi-modal information dissemination framework² in which each vehicle can receive updates about *one or more physical processes at a time*. A roadside unit (RSU) schedules updates on multiple processes such that the *average AoI and the RSU's power consumption* can be minimized at the same time. The two objectives are coupled in a conflicting manner due to the transmit power allocations.
- We develop a meta multi-objective reinforcement learning (meta-MORL) framework to minimize both the AoI at the vehicles and the RSU's power expenditure while optimizing the messages' decoding order and their corresponding power allocations. In this context, we
 - first design a hybrid DRL model, namely, hybrid deep Q-network (DQN)-deep deterministic policy gradient (DDPG) model to obtain the Pareto front of the considered multi-objective problem. The DQN solves the messages' decoding order and the DDPG handles the continuous power allocation decision. The model needs to be retrained for each point of the Pareto front.
 - then, we develop a two-stage meta-MORL solution to deal with the multiple sub-problems determined by the preference weight of the objectives and to estimate the Pareto front *without retraining*. The first stage trains a policy with a good generalization of the preference weight of the objectives. The fine-tuning stage is then applied to quickly adapt the trained policy for an unseen preference weight of the objectives.
- Extensive simulations are provided to evaluate the performance of the proposed algorithm and the generaliza-

2. The non-orthogonal multi-modal information dissemination is based on superposed message transmission from RSU and successive interference cancellation (SIC)-enabled decoding at vehicles.

tion capability of the proposed meta-MORL solution. The results demonstrate that the proposed algorithms can efficiently optimize the messages' decoding order and power allocation issues, and the meta-multi-objective RL adapts quickly to the problem instances with unseen/new objective-preference weight.

The remainder of this paper is organized as follows. Section 2 presents the system model and the performance metrics. The problem is formulated in Section 3. The proposed hybrid DQN-DDPG DRL model is introduced in Section 4 and the multi-objective meta-DRL solution is introduced in Section 5. Section 6 illustrates simulation results and Section 7 concludes the paper.

2 SYSTEM MODEL AND PERFORMANCE METRICS

This section introduces the considered system model, communication model, and performance metrics. The notations used throughout this paper are listed in Table 2.

2.1 Network Model

The considered system consists of a set $\mathcal{V} = \{v_i\}_{i=1}^V$ of V vehicles supported by an RSU that disseminates timely status updates to the vehicles. The RSU is equipped with a uniform linear array of N antennas. A multi-modal data dissemination scenario is considered, in which the RSU is capable of providing timely status updates about a set $\mathcal{F} = \{f_l\}_{l=1}^F$ of F physical processes. The payload size of an update is L bits. Each vehicle is interested in maintaining freshness of its information status about a subset of processes $\mathcal{R}_i \subseteq \mathcal{F}$. To represent the information demands of the vehicles, we define $\mathbf{R} = [r_{i,l}]_{V \times F}$ such that

$$r_{i,l} = \begin{cases} 1, & \text{if vehicle } i \text{ is interested in process } l, \\ 0, & \text{otherwise.} \end{cases} \quad (1)$$

The time is divided into T time slots each of duration δ . Let $\psi_0 = \{x_0, y_0\}$ be the coordinates of the RSU and $\psi_i^{(t)} = \{x_i^{(t)}, y_i^{(t)}\}$ be the coordinates of vehicle i at time slot t . The angle of vehicle i relative to the RSU at time slot t can be expressed as follows:

$$\phi_i^{(t)} = \arccos \frac{x_i^{(t)} - x_0}{\ell_i^{(t)}}, \quad (2)$$

where $\ell_i^{(t)} = \|\psi_i^{(t)} - \psi_0\|$ is the distance between the vehicle i and the RSU. The communication channel between the RSU and vehicle i at time slot t is modeled as follows:

$$\mathbf{h}_i^{(t)} = \sqrt{\frac{c_0}{4\pi f_c \ell_i^{(t)2}}} \mathbf{a}^H(\phi_i^{(t)}) e^{j2\pi \varrho_i^{(t)}}, \quad (3)$$

where f_c is the carrier frequency, c_0 is the speed of light, and $\varrho_i^{(t)}$ is the Doppler shift due to the movement of vehicle i expressed as $\varrho_i^{(t)} = \frac{c_i f_c \cos \phi_i^{(t)}}{c_0}$, where c_i is the speed of vehicle i [32]. Assuming a uniform linear antenna array at the RSU, the transmit array steering vector $\mathbf{a}(\phi_i^{(t)}) \in \mathbb{C}^{N \times 1}$ (with $\phi_i^{(t)}$ as the azimuth angle between the RSU and vehicle i at time slot t) can be expressed as follows:

$$\mathbf{a}(\phi_i^{(t)}) = [1, e^{j\pi \sin \phi_i^{(t)}}, e^{j2\pi \sin \phi_i^{(t)}}, \dots, e^{j(N-1)\pi \sin \phi_i^{(t)}}], \quad (4)$$

where $j = \sqrt{-1}$ and the antenna spacing is $\lambda/2$ with λ as the carrier wavelength.

TABLE 1
Existing related work.

Ref.	Year	Vehicular network	Aol	NOMA multi-modal dissemination	DRL-based solution	Hybrid DQN-DDPG	meta-DRL	Pareto front using meta-MORL
[17]	2018	✓	✓	X	X	X	X	X
[18]	2020	✓	✓	X	X	X	X	X
[5]	2020	✓	✓	X	✓	X	X	X
[19]	2020	✓	✓	X	✓	X	X	X
[2]	2022	✓	✓	X	X	X	X	X
[27]	2020	X	✓	X	X	X	X	X
[28]	2018	X	✓	X	X	X	X	X
[29]	2021	X	✓	X	X	X	X	X
[30]	2023	X	✓	X	X	X	X	X
[7]	2021	✓	X	X	✓	✓	✓	X
[31]	2022	✓	✓	X	✓	X	X	X
Ours	-	✓	✓	✓	✓	✓	✓	✓

TABLE 2
Main notations used in the paper.

Notation	Description	Notation	Description
V	Number of vehicles in the vehicles set \mathcal{V}	N	Number of antenna elements at the RSU
F	Number of physical processes in the processes set \mathcal{F}	L	Payload size of an update (in bits)
\mathcal{R}_i	Processes of interest to vehicle v_i ($\mathcal{R}_i \subseteq \mathcal{F}$)	$\mathbf{R} = [r_{i,l}]_{V \times F}$	$r_{i,l} = 1$ if vehicle v_i is interested in process f_l , $r_{i,l} = 0$ otherwise
T/δ	Number of time slots/Duration of each slot	$\psi_0 = \{x_0, y_0\}$	Coordinates of the RSU
$\psi_i^{(t)} = \{x_i^{(t)}, y_i^{(t)}\}$	Coordinates of vehicle i at time slot t	$\phi_i^{(t)}$	Angle of vehicle i relative to the RSU at time slot t
$\ell_i^{(t)}$	Distance between the vehicle i and the RSU	$\mathbf{h}_i^{(t)}$	Communication channel between the RSU and vehicle i at time slot t
$f_c/c_0/c_i$	Carrier frequency/Speed of light/Speed of vehicle i	$\theta_i^{(t)}$	Doppler shift due to the movement of vehicle i
$\mathbf{a}(\phi_i^{(t)})/\phi_i^{(t)}$	Transmit steering vector/Azimuth angle between RSU and v_i at slot t	$\boldsymbol{\pi}^{(t)}$	Decoding order decision of the messages at time slot t
$\mathbf{p}^{(t)}$	Power allocation decision at time slot t	$z_i^{(t)}/n_i$	Received signal/Additive white Gaussian noise at vehicle i
\mathbf{w}	Beamforming vector at time slot t	$\chi_i^{(t)}/\tilde{\xi}$	Large-scale channel attenuation of vehicle i /Normalization factor
$\gamma_{i,\pi_{l'}^{(t)}}^{(t)}(\boldsymbol{\pi}^{(t)}, \mathbf{p}^{(t)})$	SINR experienced at vehicle i to decode the $\pi_{l'}^{(t)}$ -th message	$\varepsilon_i^{\max}/\varepsilon_i(\gamma_i^{(t)})$	Maximum allowed error probability/Decoding error probability
$\Phi(\cdot)/\omega$	Channel dispersion/Channel bandwidth	δ_1/δ_2	Vehicles' parameters acquisition time/Information transmission time
$\Delta_{i,\pi_{l'}^{(t)}}^{(t)}/\bar{\Delta}_{i,l}$	Instantaneous Aol/Time-average Aol of f_l at vehicle i	$\bar{\Delta}^{\max}/\bar{\Delta}^{\min}$	Maximum/Minimum value of the total time-average Aol
$\bar{p}^{(t)}$	Time-average power consumption at RSU	$O(\boldsymbol{\pi}^{(t)}, \mathbf{p}^{(t)})/\zeta$	Objective function/Relative objective's preference weight
$\mathcal{S}/\mathcal{A}/\rho^{(t)}$	State space/Action space/Immediate reward	$\theta^Q/\theta^{\zeta}/\theta^\mu$	DQL network weights/Critic network weights/Actor network weights

2.2 Received Signal and SINR Model

Let $[f_1^{(t)}, f_2^{(t)}, \dots, f_F^{(t)}]$ be the raw messages of the physical processes \mathcal{F} at time slot t , the RSU sends a superposed message $\sum_{l=1}^F \sqrt{p_{\pi_l^{(t)}}^{(t)}} f_{\pi_l^{(t)}}^{(t)}$ according to a decoding order decision $\boldsymbol{\pi}^{(t)} = [\pi_1^{(t)}, \pi_2^{(t)}, \dots, \pi_F^{(t)}]$ and power allocation decision $\mathbf{p}^{(t)} = [p_1^{(t)}, \dots, p_F^{(t)}]$, where $\pi_l^{(t)}$ is the l -th elements of the decoding order decision $\boldsymbol{\pi}^{(t)}$. The RSU broadcasts the superposed message to the vehicles. Therefore, the received signal at vehicle i can be modeled as follows:

$$z_i^{(t)} = \mathbf{w}^{(t)} \left(\sum_{l=1}^F \sqrt{p_{\pi_l^{(t)}}^{(t)}} f_{\pi_l^{(t)}}^{(t)} \right) \mathbf{h}_i^{(t)H} + n_i, \quad (5)$$

where $n_i \sim \mathcal{CN}(0, \sigma^2)$ is the additive white Gaussian noise (AWGN), H denotes the Hermitian transpose, and $\mathbf{w}^{(t)}$ is the beamforming vector. The maximum ratio transmission (MRT) beamforming scheme is considered [33], in which the asymptotically optimal beamformer vector for a set of vehicles \mathcal{V} is a linear combination of channels of these vehicles [23], [34]. Consequently, the MRT beamforming vector is expressed as follows:

$$\mathbf{w}^{(t)} = \sum_{i=1}^V \frac{\mathbf{h}_i^{(t)}}{\sqrt{N \chi_i^{(t)} \tilde{\xi}}}, \quad (6)$$

where $\chi_i^{(t)} = \frac{c_0}{4\pi f_c \ell_i^{(t)}} e^{-j2\pi \theta_i^{(t)}}$ is the large-scale channel attenuation of vehicle i and $\tilde{\xi}$ is a normalization factor [23],

[35]. For a given decoding order decision $\boldsymbol{\pi}^{(t)}$, the vehicles decode the messages such that the message corresponding to the $\pi_{l'}^{(t)}$ -th physical process is decoded before the message of the $\pi_{m'}^{(t)}$ -th process, $\forall l' \leq m'$. Consequently, the signal-to-interference plus-noise ratio (SINR) experienced at vehicle i to decode the $\pi_{l'}^{(t)}$ -th message is given by

$$\gamma_{i,\pi_{l'}^{(t)}}^{(t)}(\boldsymbol{\pi}^{(t)}, \mathbf{p}^{(t)}) = \frac{p_{\pi_{l'}^{(t)}}^{(t)} |\mathbf{h}_i^{(t)H} \mathbf{w}^{(t)}|^2}{\sum_{m'=l'+1}^F p_{\pi_{m'}^{(t)}}^{(t)} |\mathbf{h}_i^{(t)H} \mathbf{w}^{(t)}|^2 + \sigma^2}, \quad \forall 1 \leq l' \leq F. \quad (7)$$

2.3 Decoding Error Probability

Note that SIC is performed at the vehicles to obtain the required updates, such that to successfully estimate the $\pi_{l'}^{(t)}$ -th message at vehicle i , it has to first perform SIC to estimate and remove all the messages $\pi_m^{(t)} \forall 1 \leq m \leq l' - 1$. Once these messages are removed, vehicle i can perform direct decoding by treating the data of messages $\pi_{l'+1}, \pi_{l'+2}, \dots, \pi_F$ as interference according to (7). Consequently, the $\pi_{l'}^{(t)}$ -th message can be estimated at vehicle i if

$$\varepsilon_i(\gamma_{i,\pi_m^{(t)}}^{(t)}(\boldsymbol{\pi}^{(t)}, \mathbf{p}^{(t)})) \leq \varepsilon_i^{\max}, \quad \forall 1 \leq m \leq l', \quad (8)$$

where ε_i^{\max} is the maximum allowed error probability at vehicle i and the decoding error probability can be expressed

as follows [36]:

$$\varepsilon_i(\gamma_{i,\pi_m}^{(t)}(\boldsymbol{\pi}^{(t)}, \mathbf{p}^{(t)})) = \Phi \left(\sqrt{\frac{\delta_2 \omega}{\Gamma_{i,\pi_m}^{(t)}}} \left[\ln \left(1 + \gamma_{i,\pi_m}^{(t)}(\boldsymbol{\pi}^{(t)}, \mathbf{p}^{(t)}) \right) - \frac{L \ln 2}{\delta_2 \omega} \right] \right), \quad (9)$$

where $\Phi(q) \triangleq \frac{1}{\sqrt{2\pi}} \int_q^\infty \exp(-\frac{u^2}{2}) du$, $\Gamma_i^{(t)} \triangleq 1 - \frac{1}{(1 + \gamma_{i,\pi_m}^{(t)}(\boldsymbol{\pi}^{(t)}, \mathbf{p}^{(t)}))^2}$ is the channel dispersion, $\gamma_{i,\pi_m}^{(t)}$ is the SINR at vehicle i at time slot t , ω is the bandwidth of the channel, and $\delta_2 \triangleq \delta - \delta_1$ is the information transmission time, with δ_1 as the dedicated time to acquire the vehicles' angular parameters (i.e., location and speed). It is worth noting that according to the SIC mechanism, for a given decoding order decision $\boldsymbol{\pi}^{(t)}$, a vehicle can correctly estimate the $\pi_{l'}^{(t)}$ -th message if all the previous messages $\pi_m^{(t)} \forall 1 \leq m \leq l' - 1$ have been correctly estimated and removed regardless of whether this vehicle is interested of previous $\pi_m^{(t)} \forall 1 \leq m \leq l' - 1$ messages or not.

2.4 Age of Information

The instantaneous AoI of the $\pi_{l'}^{(t)}$ -th physical process at vehicle i evolves according to

$$\Delta_{i,\pi_{l'}}^{(t)}(\boldsymbol{\pi}^{(t)}, \mathbf{p}^{(t)}) = \begin{cases} \delta, & \text{if (8) is satisfied,} \\ \Delta_{i,\pi_{l'}}^{(t-1)} + \delta, & \text{otherwise.} \end{cases} \quad (10)$$

The time-average AoI of f_l at vehicle i over T time slots is $\bar{\Delta}_{i,l}(\boldsymbol{\pi}^{(t)}, \mathbf{p}^{(t)}) \triangleq \mathbb{E}_T[\Delta_{i,l}^{(t)}(\boldsymbol{\pi}^{(t)}, \mathbf{p}^{(t)})] = \frac{1}{T} \sum_{t=1}^T \Delta_{i,l}^{(t)}(\boldsymbol{\pi}^{(t)}, \mathbf{p}^{(t)})$. Consequently, the total time-average AoI can be expressed as follows:

$$\begin{aligned} \bar{\Delta}(\boldsymbol{\pi}^{(t)}, \mathbf{p}^{(t)}) &= \sum_{i=1}^V \sum_{l=1}^F r_{i,l} \bar{\Delta}_{i,l}(\boldsymbol{\pi}^{(t)}, \mathbf{p}^{(t)}) \\ &= \frac{1}{T} \sum_{i=1}^V \sum_{t=1}^T \sum_{l=1}^F r_{i,l} \Delta_{i,l}^{(t)}(\boldsymbol{\pi}^{(t)}, \mathbf{p}^{(t)}). \end{aligned} \quad (11)$$

Note that the maximum value of $\bar{\Delta}_{i,l}$ is $\delta(T+1)/2$, which corresponds the case of no update about f_l is received at vehicle i over the T time slots. Thus, the maximum value (upper bound) of the total time-average AoI $\bar{\Delta}^{\max}$ can be expressed as follows:

$$\bar{\Delta}^{\max} = \frac{\delta(T+1)}{2} \sum_{i=1}^V \sum_{l=1}^F r_{i,l}, \quad (12)$$

which corresponds the case of no update is received by any vehicle during the T time slots. The minimum value (lower bound) of the total time-average AoI $\bar{\Delta}^{\min}$ corresponds the case of each vehicle is able to decode its required messages in each time slot. Consequently, $\bar{\Delta}^{\min}$ can be expressed as:

$$\bar{\Delta}^{\min} = \delta \sum_{i=1}^V \sum_{l=1}^F r_{i,l}. \quad (13)$$

2.5 A Toy Example

Fig. 1 illustrates a schematic diagram of the considered system model with $F = 4$ processes and $V = 4$ vehicles, the vehicles' information demand matrix is

$$\mathbf{R} = [r_{i,l}]_{4 \times 4} = \begin{bmatrix} f_1 & f_2 & f_3 & f_4 \\ 1 & 1 & 0 & 0 \\ 0 & 0 & 1 & 1 \\ 0 & 1 & 0 & 1 \\ 1 & 0 & 0 & 0 \end{bmatrix} \begin{matrix} v_1 \\ v_2 \\ v_3 \\ v_4 \end{matrix}. \quad (14)$$

The messages are superposed at the RSU according to a dummy decoding order decision $\boldsymbol{\pi}^{(t)} = [1, 2, 3, 4]$. Let us assume that the power is properly allocated, the SIC at the vehicles is performed as follows. At a given vehicle v_i , the message $f_1^{(t)}$ can be obtained by applying direct decoding from the received signal while treating the other messages as interference. If the condition in (8) is satisfied and $f_1^{(t)}$ is correctly decoded, the AoI of process f_1 at vehicle v_i will be updated if $r_{i,1} = 1$ (i.e., process f_1 is of interest to v_i). The SIC procedure is performed to get message $f_2^{(t)}$ if the previous message $f_1^{(t)}$ was correctly decoded, such that $f_1^{(t)}$ is removed and $f_3^{(t)}$ and $f_4^{(t)}$ are treated as interference, and so on. It is worth noting that the iterations of the SIC at each vehicle depends on its requirements and the decoding order decision $\boldsymbol{\pi}^{(t)}$. For example, in Fig. 1 vehicle v_1 applies direct decoding to get $f_1^{(t)}$ and one SIC iteration to get $f_2^{(t)}$, vehicles v_2 and v_3 apply direct decoding followed by three SIC iterations to get $f_4^{(t)}$, and vehicle v_4 applies only the direct decoding to get $f_1^{(t)}$.

It is also worth mentioning that, unlike the conventional NOMA scenarios where the messages can be superposed according to the ranking of the communication channel conditions, both the power allocation and the decoding order decision $\boldsymbol{\pi}^{(t)}$ should be optimized to consider the vehicles demands and the value of the AoI at each vehicle.

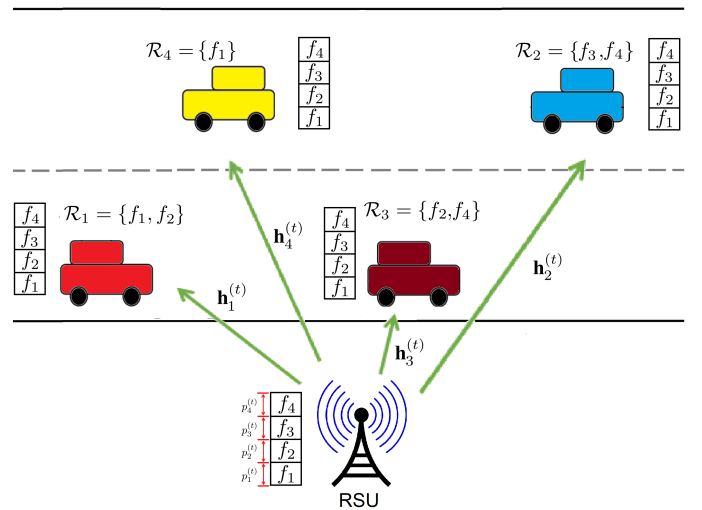


Fig. 1. System model with $V = 4$ vehicles, $F = 4$ processes, information demand \mathbf{R} in (14), and a decoding order decision $\boldsymbol{\pi}^{(t)} = [1, 2, 3, 4]$.

3 MULTI-OBJECTIVE PROBLEM STATEMENT

We consider minimizing the time-average AoI of each process at the vehicles $\bar{\Delta}(\boldsymbol{\pi}^{(t)}, \mathbf{p}^{(t)})$ as well as the time-average power consumption at RSU, $\bar{p}^{(t)} = \frac{1}{T} \sum_{t=1}^T \sum_{l=1}^F p_l^{(t)}$. The multi-objective problem is thus formulated as follows:

$$\mathbf{P1} \quad \min_{\boldsymbol{\pi}^{(t)}, \mathbf{p}^{(t)}} \left\{ \bar{\Delta}(\boldsymbol{\pi}^{(t)}, \mathbf{p}^{(t)}), \bar{p}^{(t)} \right\} \quad (15a)$$

$$\text{s.t.} \quad \sum_{l=1}^F p_l^{(t)} \leq P^{\max}, \quad (15b)$$

$$p_l^{(t)} \geq 0, \quad \forall 1 \leq l \leq F, \quad (15c)$$

$$\pi_{l'}^{(t)} \in \mathcal{F}, \quad \forall 1 \leq l' \leq F, \quad (15d)$$

$$\text{card}(\boldsymbol{\pi}^{(t)}) \leq F. \quad (15e)$$

Constraints (15b) and (15c) guarantee that the allocated power is positive and less than the maximum transmission power of the RSU. Constraint (15d) guarantees that the decoding order decision captures only the physical processes and (15e) guarantees there is no repeated processes, with $\text{card}(\cdot)$ as a cardinality operator.

Keeping in mind the trade-off between these two objectives and the fact that they have different units, ranges, and orders of magnitude, they should be normalized such that they have similar ranges [12]. The common strategy to handle multi-objective optimization is to convert the problem into a single objective optimization problem, which can be implemented using three approaches. The first approach referred to as ϵ -constraint approach, in which one objective is selected to be the primary objective and the others appear as constraints with respect to the auxiliary parameter ϵ [9]. This approach has three major shortcomings: (i) The value of the auxiliary parameter ϵ should be carefully adjusted as it may affect the problem feasibility; (ii) The selection of the primary objective function; (iii) More than one auxiliary parameter may be required to constrain objectives of different ranges. The second approach is Tchebycheff approach, in which the primary objective is to optimize (maximize or minimize) an auxiliary parameter and all objectives appear as weighted constraints with respect to the auxiliary parameter [10]. The third approach is the weighted sum, in which the objectives are combined into a single function using prefixed weights [11], [12], [13].

The weighted-sum is an effective approach to handle a multi-objective optimization problem, where each weight corresponds to a particular sub-problem. The solutions of J sub-problems constitute a set of the Pareto optimal solutions or the Pareto optimal front [37].

Definition 1. Let \mathcal{X} represents the feasible space of the optimization problem

$$\min_{\mathbf{x}} \mathbf{o}(\mathbf{x}) = \{o_1(\mathbf{x}), o_2(\mathbf{x}), \dots, o_K(\mathbf{x})\} \quad \text{subject to: } \mathbf{x} \in \mathcal{X}$$

A point $\mathbf{x}^* \in \mathcal{X}$ is a Pareto optimal point if and only if there does not exist another point, $\mathbf{x} \in \mathcal{X}$, such that $\mathbf{o}(\mathbf{x}) \leq \mathbf{o}(\mathbf{x}^*)$, and $o_k(\mathbf{x}) < o_k(\mathbf{x}^*)$ for at least one objective function. The set of all Pareto optimal points is called the Pareto frontier.

To obtain the Pareto optimal fronts for (15), we consider the normalized weighted metric method, which entails minimizing the difference between the objectives and the

corresponding utopia solutions. Fortunately, we can obtain both the Utopia and Nadir solutions of the two objectives. The Utopia and Nadir solutions of time-average AoI are $\bar{\Delta}^{\max}$ and $\bar{\Delta}^{\min}$ as expressed in (12) and (13), respectively. While for the time-average power consumption, the Nadir and Utopia solutions are the maximum transmission power of the RSU P^{\max} and the minimum transmission power of the RSU ($P^{\min} = 0$), respectively. Consequently, we define the objective function as:

$$O(\boldsymbol{\pi}^{(t)}, \mathbf{p}^{(t)}) = \zeta \frac{\bar{\Delta}(\boldsymbol{\pi}^{(t)}, \mathbf{p}^{(t)}) - \bar{\Delta}^{\min}}{\bar{\Delta}^{\max} - \bar{\Delta}^{\min}} + (1 - \zeta) \frac{\bar{p}^{(t)} - P^{\min}}{P^{\max} - P^{\min}}, \quad (16)$$

where $0 \leq \zeta \leq 1$ is a relative weight to give preference to minimize the AoI or the power. It is worth noting that the objective function in (16) is dimensionless, bounded by $[0, 1]$, and the decision-maker can set the objective-preference weight to any desired value $0 \leq \zeta \leq 1$. This is not the case in other multi-objective optimization methods, such as ϵ -constraint method, in which the value of ϵ should be selected carefully to avoid infeasibility issues.

Henceforth, the multi-objective optimization problem **P1** can be transformed as follows:

$$\mathbf{P2} \quad \min_{\boldsymbol{\pi}^{(t)}, \mathbf{p}^{(t)}} O(\boldsymbol{\pi}^{(t)}, \mathbf{p}^{(t)}) \quad (17a)$$

$$\text{s.t.} \quad (15b) - (15e). \quad (17b)$$

The optimization problem in (17) is a mixed-integer non-linear programming (MINLP) problem that involves discrete (decoding order decision $\boldsymbol{\pi}^{(t)}$) and continuous (power allocation $\mathbf{p}^{(t)}$) decision making over multiple transmission time slots. Conventional optimization methods are not appropriate for solving the problem (17) which evolves over time, hence we resort to the DRL strategies for solving problem (17).

4 HYBRID DQN-DDPG -BASED DRL SOLUTION

In this section, a hybrid DQN-DDPG DRL model is introduced to solve the optimization problem in (17) for a given value of the objective-preference weight ζ .

4.1 Theoretical Preliminaries

Reinforcement learning is the process of learning by an agent to maximize the discounted reward over the learning time horizon by interacting with an environment. At each learning epoch, given the current state of the environment, an action is performed by the agent on the environment which transits to the next state and returns an immediate reward. A key metric in training the agent is the Q -function which estimates the future reward of taking an action \mathbf{a} at a given state \mathbf{s} . It has been shown that learning based on Q -function (also referred to as Q -learning) converges towards an optimal solution after visiting each state-action pair with sufficient number of learning iterations [38]. Such a learning approach is impractical in the following scenarios: (1) The number of state-action pairs is very large; (2) The action space and/or state space are/is continuous. Utilizing deep neural networks (DNN) to approximate the Q -function is

referred to as DRL, in which the Q -function is written as $Q(s, \mathbf{a} \mid \theta)$, where θ represents the weight vector of the DNN [39]. Actor-critic networks comprising of two deep Q -learning networks are able to deal with environments that have continuous action spaces [40]. DDPG is an actor-critic algorithm involves two networks, namely, the actor and critic networks. The actor network learns to obtain the best action at a given state, while the critic evaluates the reward of the state-action pair [40].

It is worth mentioning that the DRL model is commonly formulated as a Markov Decision Process (MDP) problem. An MDP is represented by a tuple $\{\mathcal{S}, \mathcal{A}, \vartheta, \rho\}$, where \mathcal{S} is the state space that consists of the set of all possible states, \mathcal{A} is a finite set of actions from which the agent can choose, $\vartheta : \mathcal{S} \times \mathcal{A} \times \mathcal{S} \rightarrow [0, 1]$ is a transition probability which defines the probability of observing a state after executing an action at a given environment's state, and $\rho : \mathcal{S} \times \mathcal{A} \rightarrow \mathbb{R}$ is the expected reward of performing an action at a given state. We note that discretizing continuous action space increases the problem's dimensionality. Thus, DDPG [40] is applied to handle continuous action space. The DDPG algorithm maintains a parameterized actor policy, which maps states to a probability distribution over the actions [40]. In this context, a hybrid DQN-DDPG DRL model is developed such that the DQN handles the decoding order decision (discrete value) and the actor-critic DDPG handles the power allocation (continuous value) decision. The following section defines the state space, action space, and reward of the designed DRL model.

4.2 DRL Model

Our goal is to design a DRL system that jointly optimizes the decoding order decision (discrete value) and the power allocation (continuous value) decision to minimize the objective function in (17). In this context, we develop a DRL model that involves the definition of the environment state, the action, and the immediate reward function $\rho^{(t)}$ as follows:

4.2.1 The Environment State Space

The state space is denoted as \mathcal{S} , in which the state at time slot t captures the communication channel between the RSU and the vehicles as well as the AoI of the required processes at the vehicles. Thus, the state at time slot t is given by

$$\mathbf{s}^{(t)} = \left\{ \left\{ \sum_{i=1}^V r_{i,l} \chi_i^{(t)} \right\}, \left\{ \sum_{i=1}^V r_{i,l} \Delta_{i,l}^{(t)} \right\} \right\}_{l=1}^F. \quad (18)$$

4.2.2 Action Space

At each decision-making instant, based on the observed state, the DQN and actor-critic models make an action to order the physical process for encoding and to allocate the power, respectively. Under this setup, the action space \mathcal{A} represents pairs of actions $\mathbf{a}^{(t)} = (\mathbf{a}_\pi^{(t)}, \mathbf{a}_P^{(t)})$, such that

- $\mathbf{a}_\pi^{(t)} = [\pi_1^{(t)}, \pi_2^{(t)}, \dots, \pi_F^{(t)}]$ is the decoding order decision which is obtained using the DQN agent.
- $\mathbf{a}_P^{(t)} = [\alpha_1^{(t)}, \alpha_2^{(t)}, \dots, \alpha_F^{(t)}] P^{max}$ is the power allocation decision, with $\alpha^{(t)} = [\alpha_1^{(t)}, \alpha_2^{(t)}, \dots, \alpha_F^{(t)}]$ as the output of the actor-critic/DDPG agent.

4.2.3 Reward

Based on the observed state and the agents' action, an immediate reward is returned by the environment that reflects the suitability of the action to minimize the objective function with a given value of the objective preference weight. For the considered optimization problem, a good decision on process decoding order and power allocation can minimize the AoI and power consumption with the given preference weight ζ . To reflect the quality of the action taken by the agents, the immediate reward at time slot t is expressed as:

$$\rho^{(t)} = \exp \left(-\zeta \frac{\bar{\Delta}_t(\boldsymbol{\pi}^{(t)}, \mathbf{p}^{(t)}) - \bar{\Delta}^{\min}}{\bar{\Delta}_t^{\max} - \bar{\Delta}^{\min}} - (1 - \zeta) \frac{\hat{p}^{(t)} - P^{\min}}{P^{\max} - P^{\min}} \right) - \Upsilon^{(t)}, \quad (19)$$

where $\Upsilon^{(t)} = \kappa [\sum_{l=1}^F \alpha_l^{(t)} - 1]^+$ is a penalty function with $[x]^+ = \max\{x, 0\}$ and κ as a penalty constant, $\hat{p}^{(t)} = \frac{1}{t} \sum_{t'=1}^t \sum_{l=1}^F p_l^{(t')}$, $\bar{\Delta}_t(\boldsymbol{\pi}^{(t)}, \mathbf{p}^{(t)})$, and $\bar{\Delta}_t^{\max}$, are obtained by replacing T by t in (11) and (12), respectively. It is worth noting that the parameters in equation (16) are redefined in (19) to represent the AoI and power consumption at time instant t . Keeping in mind that our aim is to minimize the objective function, while the DRL learns to maximize the accumulative reward, the exponential function is chosen to define the immediate reward which stabilizes the offline training [5]. Finally, $\Upsilon^{(t)}$ represents a penalty of violating the constraint (15b).

4.3 Hybrid DQN-DDPG Algorithm

A schematic block diagram of the proposed hybrid DQN-DDPG DRL model is shown in Fig. 2, which illustrates the action-making agents for decoding order and power allocation as well as the learning process for both agents for a given value of the objective-preference weight ζ . The training algorithm of the hybrid DQN-DDPG model is illustrated in **Algorithm 1**. The objective-preference weight ζ , and DQN weights θ^Q , critic network weights θ^{Q_c} , actor network weights θ^μ are the input of the algorithm. For each training episode, the environment is initialized and an initial state is obtained (line 4). At every time step t , the DQN model obtains a decoding order action $\mathbf{a}_\pi^{(t)}$ using the $\bar{\epsilon}$ -greedy policy to balance the exploitation of known actions and the exploration of new actions (line 6). The DDPG model obtains a power allocation action $\mathbf{a}_P^{(t)}$ using the actor network $\mu(\mathbf{s}^{(t)} \mid \theta^\mu)$ (lines 7-8). A combined action $\mathbf{a}^{(t)} = (\mathbf{a}_\pi^{(t)}, \mathbf{a}_P^{(t)})$ is applied on the environment which returns an immediate reward $\rho^{(t)}$ and transits to a new state $\mathbf{s}^{(t+1)}$ (line 9). The transition tuple $\{\mathbf{s}^{(t)}, \mathbf{a}^{(t)}, \rho^{(t)}, \mathbf{s}^{(t+1)}\}$ is added to the replay buffer **B** (line 10). A mini-batch of transitions are sampled from the replay buffer to update the deep networks (line 12).

The *Adam* optimizer [41] is considered to update the weights of the DNNs with an aim to minimize the following loss functions

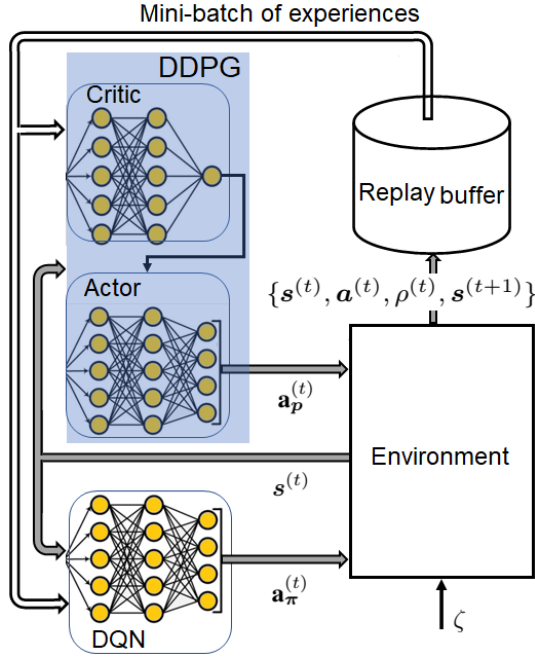


Fig. 2. Hybrid DQN-DDPG model for age-optimum information dissemination.

Algorithm 1 Hybrid DQN-DDPG training algorithm for age-optimum information dissemination.

- 1: **Input:** Objective-preference weight ζ , No. of episodes, DQL network weights θ^Q , critic network weights θ^{Q_c} , and actor network weights θ^μ ;
- 2: Initialize target network $\theta^{Q'} \leftarrow \theta^Q$, $\theta^{Q'_c} \leftarrow \theta^{Q_c}$, and $\theta^{\mu'} \leftarrow \theta^\mu$;
- 3: **For** $episode = 1$ **to** No. of episodes **do**
- 4: Initialize the environment and receive the initial state $s^{(1)}$;
- 5: **Repeat:**
- 6: With probability $\bar{\epsilon}$, select randomly an action $\mathbf{a}_\pi^{(t)} \in \mathcal{A}_\pi$; Otherwise, select $\mathbf{a}_\pi^{(t)} = \arg \max_{\forall \mathbf{a}_\pi^{(t)} \in \mathcal{A}_\pi} Q(s^{(t)}, \mathbf{a}_\pi^{(t)} | \theta^Q)$;
- 7: Obtain $\boldsymbol{\alpha}^{(t)} = [\alpha_1^{(t)}, \alpha_2^{(t)}, \dots, \alpha_F^{(t)}] \triangleq \mu(s^{(t)} | \theta^\mu) + N$, where N is the exploration noise [40];
- 8: Obtain the power allocation action $\mathbf{a}_P^{(t)} = \boldsymbol{\alpha}^{(t) P^{max}}$;
- 9: Observe the reward $\rho^{(t)}$ using (19) and next state $s^{(t+1)}$ by applying the action $\mathbf{a}^{(t)} = (\mathbf{a}_\pi^{(t)}, \mathbf{a}_P^{(t)})$;
- 10: Store the transition $\{s^{(t)}, \mathbf{a}^{(t)}, \rho^{(t)}, s^{(t+1)}\}$ in \mathbf{B} ; $t = t + 1$;
- 11: **Until** terminal state $t = T$;
- 12: Sample a mini-batch of M transitions from \mathbf{B} ;
- 13: Update the weight θ^Q , θ^{Q_c} and θ^μ by minimizing the corresponding loss functions in (20);
- 14: Update the target networks

$$\begin{aligned} \theta^{Q'} &\leftarrow \tau \theta^Q + (1 - \tau) \theta^{Q'}, \\ \theta^{Q'_c} &\leftarrow \tau \theta^{Q_c} + (1 - \tau) \theta^{Q'_c}, \\ \theta^{\mu'} &\leftarrow \tau \theta^\mu + (1 - \tau) \theta^{\mu'}. \end{aligned}$$

15: **End for**

$$\begin{aligned} L(\theta^Q) &= \sum_t (\rho^{(t)} + \max_{\forall \mathbf{a}'_\pi \in \mathcal{A}} Q'(s', \mathbf{a}'_\pi, \theta^{Q'}) - Q(s^{(t)}, \mathbf{a}_\pi^{(t)}, \theta^Q))^2, \\ L(\theta^{Q_c}) &= \sum_t (y^{(t)} - Q(s^{(t)}, \mathbf{a}_P^{(t)}, \theta^{Q_c}))^2, \\ L(\theta^\mu) &= -Q(s^{(t)}, \mathbf{a}_P^{(t)}, \theta^{Q_c}, \theta^\mu), \end{aligned} \quad (20)$$

where $y^{(t)} = \rho^{(t)} + Q'_c(s', \mathbf{a}'_\pi, \theta^{Q'_c})$ [40].

It is worth noting that both the DQN and DDPG agents work jointly such that they observe the same observation or environment state and the shared reward is not sparse and its value depends on the actions of both agents, which prevents a lazy agent situation. In other words, let us assume that the DQN model tends to become a lazy agent. In such a case, the reward of DQN model will decrease and the DDPG will not be able to compensate this behavior, i.e., cannot force the DQN model to learn a good policy. The same applies if the DDPG model tends to become a lazy agent, then it will not take advantage of the successful actions of DQN. That is, if the action of the DDPG is bad the reward will decrease regardless of how good is the action of DQN model. Such a joint effect of the actions of the two agents on the value of the reward and the shared environment observation prevent both agents from becoming a lazy agent, which may arise due to partial observability [42], [43] or sparse reward scenarios [44]."

5 META REINFORCEMENT LEARNING

In Section 4, a hybrid DQN-DDPG DRL model has been developed to solve the age-optimum information dissemination in vehicular networks problem. However, it is worth noting that a predetermined objective-preference weight is required before training the model. Consequently, the quality of the inferred solution depends on whether the objective-preference weight has been observed during the training stage. If an unseen objective-preference weight is encountered, a new model should be trained from scratch which is inefficient approach to construct the Pareto front as it requires a large number of models to be trained and stored. Inspired by recently proposed algorithms for fast adaptation in DRL models [14], [15], this section introduces a meta reinforcement learning approach to increase the diversity and quality of the solutions. The training of the meta RL is performed based on the multi step model-agnostic meta-learning (MAML) approach [45], which consists two nested stages. The inner stage performs multiple gradient descent steps to update the deep networks parameters for a given value of the relative weight, while the outer stage enables the updating of the deep networks' parameters over all the sampled values of relative weight.

5.1 Meta Reinforcement Algorithm

Training the meta-DRL model is an important part of the meta-based algorithm as it yields the parameters for the neural network that can adapt quickly to a new task. The goal of meta-learning is to ensure that the meta-based model is capable of optimizing the objective function with any objective-preference weight after a small number of fine-tuning updates. Suppose a set J tasks³ are available for learning and the corresponding objective-preference weights are sampled based on a probability distribution Λ , the j -th task is associated with loss functions $L_j(\tilde{\theta}^Q)$, $L_j(\tilde{\theta}^{Q_c})$, and $L_j(\tilde{\theta}^\mu)$ parameterized by the DQL network weights $\tilde{\theta}^Q$, critic network weights $\tilde{\theta}^{Q_c}$, and actor network

3. Each task is a scalar optimization sub-problem with an objective-preference weight

weights $\tilde{\theta}^\mu$, respectively. MAML approach guarantees convergence [45], which aims at finding good initial parameters $(\tilde{\theta}^{Q^*}, \tilde{\theta}^{Q_c^*}, \tilde{\theta}^{\mu^*})$ such that after observing a new task, a few gradient descent steps (fine-tuning steps) starting from such initial parameters can efficiently approach the optimizer of the corresponding loss functions. The multi-step MAML consists of two nested stages, the inner stage performs multiple gradient descent steps for each individual task, while the meta parameters over all the sampled tasks are updated using the outer stage. These two nested stages provide diverse and representative training, which mitigates the bias in the training [45]. Consequently, the inner stage of each task initializes at the meta parameters, (i.e., $\tilde{\theta}_{j_0}^Q = \tilde{\theta}^Q$, $\tilde{\theta}_{j_0}^{Q_c} = \tilde{\theta}^{Q_c}$, $\tilde{\theta}_{j_0}^\mu = \tilde{\theta}^\mu$) and runs M gradient descent steps as

$$\begin{aligned}\tilde{\theta}_{j_{k+1}}^Q &= \tilde{\theta}_{j_k}^Q - \alpha_Q \nabla L_j(\tilde{\theta}_{j_k}^Q), \\ \tilde{\theta}_{j_{k+1}}^{Q_c} &= \tilde{\theta}_{j_k}^{Q_c} - \alpha_{Q_c} \nabla L_j(\tilde{\theta}_{j_k}^{Q_c}), \\ \tilde{\theta}_{j_{k+1}}^\mu &= \tilde{\theta}_{j_k}^\mu - \alpha_\mu \nabla L_j(\tilde{\theta}_{j_k}^\mu),\end{aligned}\quad (21)$$

where α_Q , α_{Q_c} , and α_μ represent the inner step size of the DQL, critic, and actor networks, respectively. Consequently, the overall meta goal is given by

$$\begin{aligned}\min_{\tilde{\theta}^Q} \mathcal{L}(\tilde{\theta}^Q) &:= \mathbb{E}_{j \sim \Lambda} \left[\mathcal{L}_j(\tilde{\theta}^Q) \right] := \mathbb{E}_{j \sim \Lambda} \left[L_j(\tilde{\theta}_{j_M}^Q(\tilde{\theta}^Q)) \right], \\ \min_{\tilde{\theta}^{Q_c}} \mathcal{L}(\tilde{\theta}^{Q_c}) &:= \mathbb{E}_{j \sim \Lambda} \left[\mathcal{L}_j(\tilde{\theta}^{Q_c}) \right] := \mathbb{E}_{j \sim \Lambda} \left[L_j(\tilde{\theta}_{j_M}^{Q_c}(\tilde{\theta}^{Q_c})) \right], \\ \min_{\tilde{\theta}^\mu} \mathcal{L}(\tilde{\theta}^\mu) &:= \mathbb{E}_{j \sim \Lambda} \left[\mathcal{L}_j(\tilde{\theta}^\mu) \right] := \mathbb{E}_{j \sim \Lambda} \left[L_j(\tilde{\theta}_{j_M}^\mu(\tilde{\theta}^\mu)) \right].\end{aligned}\quad (22)$$

Then the outer stage of meta update is gradient descent steps to minimize (22). In [45], a simplified form of gradient of the losses has been derived using the chain rule, which can be expressed as

$$\begin{aligned}\nabla \mathcal{L}_j(\tilde{\theta}^Q) &= \left[\prod_{k=0}^{M-1} (1 - \alpha_Q \nabla^2 L_j(\tilde{\theta}_{j_k}^Q)) \right] \nabla L_j(\tilde{\theta}_{j_M}^Q), \\ \nabla \mathcal{L}_j(\tilde{\theta}^{Q_c}) &= \left[\prod_{k=0}^{M-1} (1 - \alpha_{Q_c} \nabla^2 L_j(\tilde{\theta}_{j_k}^{Q_c})) \right] \nabla L_j(\tilde{\theta}_{j_M}^{Q_c}), \\ \nabla \mathcal{L}_j(\tilde{\theta}^\mu) &= \left[\prod_{k=0}^{M-1} (1 - \alpha_\mu \nabla^2 L_j(\tilde{\theta}_{j_k}^\mu)) \right] \nabla L_j(\tilde{\theta}_{j_M}^\mu),\end{aligned}\quad (23)$$

where $\nabla L_j(\cdot)$ and $\nabla^2 L_j(\cdot)$ represent the gradient and Hessian operators of the loss function $L_j(\cdot)$, respectively. Finally, the full gradient descent step of the outer stage can be expressed as

$$\begin{aligned}\tilde{\theta}_{k'+1}^Q &= \tilde{\theta}_{k'}^Q - \beta_Q \mathbb{E}_{j \sim \Lambda} \nabla \mathcal{L}_{j,k'}(\tilde{\theta}^Q), \\ \tilde{\theta}_{k'+1}^{Q_c} &= \tilde{\theta}_{k'}^{Q_c} - \beta_{Q_c} \mathbb{E}_{j \sim \Lambda} \nabla \mathcal{L}_{j,k'}(\tilde{\theta}^{Q_c}), \\ \tilde{\theta}_{k'+1}^\mu &= \tilde{\theta}_{k'}^\mu - \beta_\mu \mathbb{E}_{j \sim \Lambda} \nabla \mathcal{L}_{j,k'}(\tilde{\theta}^\mu),\end{aligned}\quad (24)$$

where β_Q , β_{Q_c} , and β_μ represent the outer step size of the DQL, critic, and actor networks, respectively.

The meta-learning algorithm is illustrated in **Algorithm 2**, in which at the k -th inner stage iteration a training set of transition tuples is sampled and utilized to update the

Algorithm 2 The meta-learning algorithm for age-optimum information dissemination.

- 1: **Input:** Distribution over the objective-preference weight Λ , number of meta-learning iterations, number of sampled tasks J ;
- 2: Initialize the DQL network weights $\tilde{\theta}^Q$, critic network weights $\tilde{\theta}^{Q_c}$, and actor network weights $\tilde{\theta}^\mu$;
- 3: **For** $k' = 0$ **to** No. of meta-learning iterations **do**
- 4: Sample J tasks by distribution Λ ;
- 5: **For** $j = 1$ **to** J **do**
- 6: **For** $k = 0$ **to** M **do**
- 7: Obtain a training set of transition tuples;
- 8: Update the DRL networks parameters using (21);
- 9: **End for**
- 10: **End for**
- 11: Update the DRL networks parameters using (24);
- 12: **End for**
- 13: **Output** $\tilde{\theta}^{Q^*} \leftarrow \tilde{\theta}^Q$; $\tilde{\theta}^{Q_c^*} \leftarrow \tilde{\theta}^{Q_c}$; $\tilde{\theta}^{\mu^*} \leftarrow \tilde{\theta}^\mu$.

Algorithm 3 Fine-tuning algorithm to obtain the Pareto front using the meta-model.

- 1: **Input:** The objective-preference vector of the Pareto front $\zeta = [\zeta_1, \zeta_2, \dots, \zeta_j]$, number of fine-tuning iterations, well-trained meta-model DQL network weights $\tilde{\theta}^{Q^*}$, well-trained meta-model critic network weights $\tilde{\theta}^{Q_c^*}$, and well-trained meta-model actor network weights $\tilde{\theta}^{\mu^*}$;
- 2: **For** $j = 1$ **to** J **do**
- 3: $\theta_j^Q, \theta_j^{Q_c}, \theta_j^\mu \leftarrow \tilde{\theta}^{Q^*}, \tilde{\theta}^{Q_c^*}, \tilde{\theta}^{\mu^*}$;
- 4: **For** $episode = 1$ **to** No. of fine-tuning steps **do**
- 5: $(\theta_j^Q, \theta_j^{Q_c}, \theta_j^\mu) \leftarrow$ Hybrid DQN-DDPG($\zeta_j, \theta_j^Q, \theta_j^{Q_c}, \theta_j^\mu$) using Algorithm 1;
- 6: **End for**
- 7: Estimate the j -th Pareto point using $\theta_j^Q, \theta_j^{Q_c}, \theta_j^\mu$, and ζ_j ;
- 8: **End for**
- 9: **Output** the Pareto points.

meta parameters using (21). At the k' -th outer stage iteration, two training sets of transition tuples are independently sampled and utilized to estimate the gradient and Hessian of the loss and update meta parameters using (24).

5.2 Fine-tuning and Inference

In the meta-training stage, we have learned the initial networks parameters, which have good generalization ability. Pareto solution for any objective-preference weight can be inferred from the well-trained meta-model after undergoing a few fine-tuning steps. **Algorithm 3** illustrates how to infer a Pareto frontier of J Pareto points corresponding to a set of objective-preference weights $\zeta = [\zeta_1, \zeta_2, \dots, \zeta_j]$.

6 SIMULATION RESULTS AND DISCUSSIONS

This section introduces simulation results to evaluate the proposed framework and solution approaches.

6.1 Simulation Parameters

Without loss of generality, the considered vehicular network consists of a segment of a two-lane road along the x-axis and the vehicles move along the positive or negative directions of the x-axis. The length of the road segment is 3 km and the width of each lane is 3 m. The RSU is located at $\{1500, 50\}$ m and the vehicles' are initialized randomly on the road in both directions. The vehicles' speeds are randomly drawn from $U(10, 15)$ m/s. The initial value of the instantaneous AoI of each process of interest at each vehicle is δ . Unless

TABLE 3
Simulation Parameters.

Parameter	Value	Parameter	Value	Parameter	Value
p^{\max}	0 dB	c_i	$\sim U(10, 15)$ m/s [32]	ω	10 MHz [32]
f_c	3 GHz [32]	N	64 [32]	L	128 byte
ε^{\max}	10^{-6}	c_0	2.99×10^8 m/s	σ^2	0.1

otherwise stated, the considered values of the system parameters are listed in Table 3. The implementation of the DQN and DDPG networks involve three hidden layers of 512, 256, and 128 neurons, respectively. Each layer is followed with a rectified linear unit (ReLU) activation function. The learning rates of the DQN, actor, and critic networks are 0.001, 0.0001, and 0.001, respectively. The mini-batch size for training the hybrid DQN-DDPG model is 64, the discount factor is 0.5, and the penalty constant is 1. The number of training episodes is 1000. For the meta training, the inner step sizes of the DQL, critic, and actor networks are $\alpha_Q = 0.1$, $\alpha_{Q_c} = 0.01$, and $\alpha_\mu = 0.001$ while the outer step sizes are $\beta_Q = 0.01$, $\beta_{Q_c} = 0.01$, and $\beta_\mu = 0.001$, respectively. The number of meta learning episodes is 500 and the number of gradient descent steps and fine-tuning steps is 50. Fig. 3 shows the learning curves for the hybrid DQN-DDPG DRL model versus the number of training episodes. It can be noticed that the reward gradually increases, and its average value saturates after sufficient training episodes without a major drop in the average reward. This indicates that the adopted training parameters provide stable learning without over-fitting.

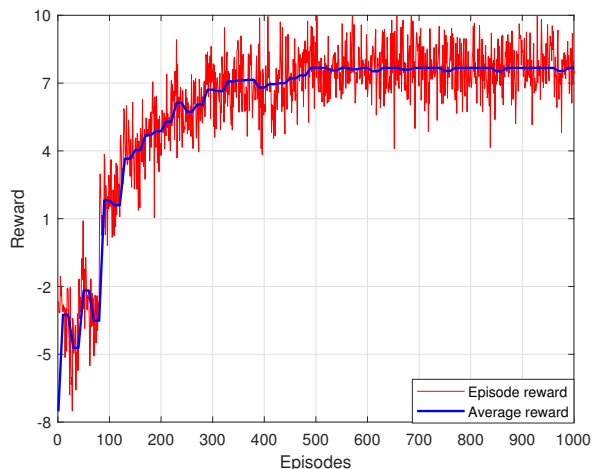


Fig. 3. The learning curves for the hybrid DQN-DDPG DRL model versus the number of training episodes.

6.2 Results

We compare the performance of the following approaches:

- *Hybrid DQN-DDPG DRL* which represents the results of the proposed DRL algorithm described in **Algorithm 1** that requires a value of the object-preference weight ζ .
- *The meta-DRL* which represents the results of the proposed meta-DRL algorithm described in **Algorithm 2**, **without** the fine-tuning step.

- *The meta-DRL with fine-tuning* which represents the results of the proposed meta-DRL algorithm described in Section 5.2 with the fine-tuning stage in **Algorithm 3**.
- *The random solution* in which the decoding order and power allocation decisions are randomly selected.
- *The exhaustive search solution* in which the power allocation decision is discretized into 10 levels and all the combinations of the decoding order and the discretized power allocation decisions are examined.

Figure 4 illustrates the objective function versus the objective-preference weight ζ for the proposed framework obtained using the four solution approaches. It is seen that the hybrid DQN-DDPG approach achieves near-optimum performance in comparison with the exhaustive search solution and the random approach provides the worst performance. The performance of the meta-based DRL is better than that of the random solution and the fine-tuning stage improves the performance of the meta-based model and provides close to optimum solutions. It is worth mentioning that a hybrid DQN-DDPG model is trained for each value of ζ in Fig. 4.

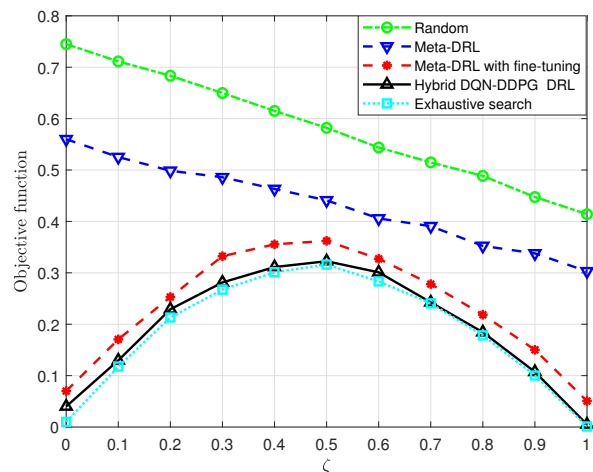


Fig. 4. Objective function in (16) versus the relative weight ζ with $V = 10$ vehicles, $F = 4$ processes and $|\mathcal{R}_i| = 2$.

To get more insight into this result, Fig. 5 illustrates the corresponding average AoI and power consumption versus ζ . It is noticed that the proposed framework provides a good trade-off between AoI and power expenditure as for low values of ζ it minimizes the power expenditure and as ζ increases it minimizes the AoI. The trade-off provided by the hybrid DQN-DDPG is close to that of the exhaustive search and the meta-DRL with fine-tuning provides a remarkably good performance. That is not the case for the random solution, in which both the AoI and power expenditure are not function of the relative weight. It is worth noting the meta-DRL solution also not a function of ζ and its performance is better than the random solution, as it is trained to minimize the objective function for randomly sampled objective-preference weights.

Figure 6 illustrates the Pareto fronts obtained by the four solution approaches. It can be noticed that the hybrid DQN-DDPG and the meta-DRL with fine-tuning approaches pro-

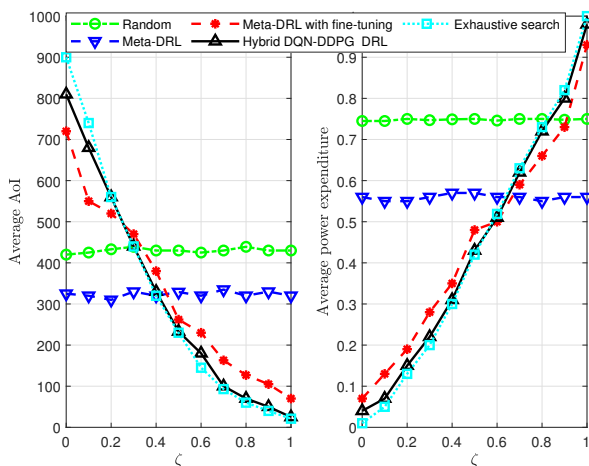


Fig. 5. Average AoI and power expenditure versus the relative weight ζ with $V = 10$ vehicles, processes $F = 4$ processes and $|\mathcal{R}_i| = 2$.

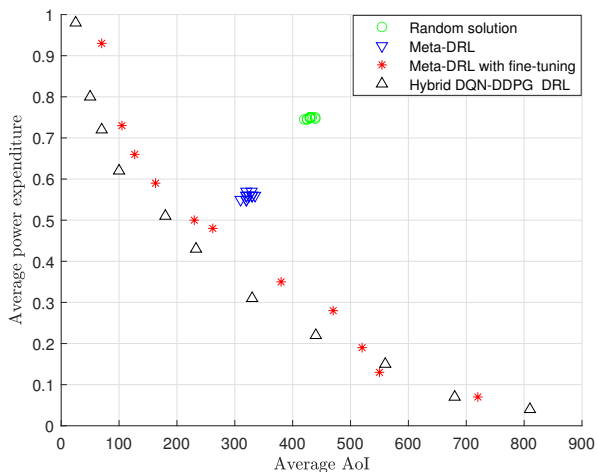


Fig. 6. Pareto fronts with $V = 10$ vehicles, $F = 4$ processes, $|\mathcal{R}_i| = 2$, and $\zeta = 0 : 0.1 : 1$.

vide non-dominated solutions constitute diverse and evenly spread of Pareto fronts, which gives the decision-maker a set of satisfactory trade-off solutions. That is not the case for the random and meta-DRL approaches where the Pareto points are concentrated in close-proximity apart from the lower left part of the figure. To quantify the quality of the Pareto fronts in Fig. 6, the hypervolume indicator (Lebesgue measure) of each Pareto front is calculated using Monte-Carlo approximation. The hypervolume indicator maps the set of points in a Pareto front to a single real value measure that represents the region dominated by that Pareto front and bounded above (for minimization problems) by a given reference point [46]. The higher the value of the hypervolume indicator the better the Pareto front to give the decision-maker satisfactory trade-off solutions. Assuming the upper bound of the two objectives as a reference point i.e., (average AoI = $\bar{\Delta}^{\max}$, average power = P^{\max}), the hypervolume indicators of the random, meta-DRL, meta-

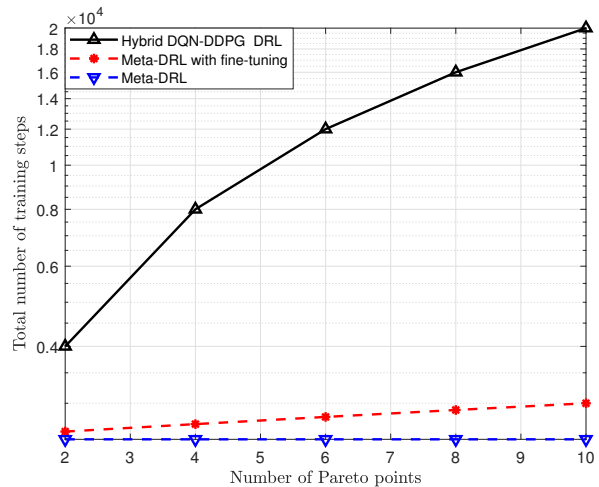


Fig. 7. Total training steps to obtain the Pareto front.

DRL with fine-tuning, and hybrid DQN-DDPG approaches in Fig. 6 equal **150**, **315**, **660**, and **710**, respectively. It is worth mentioning that the desirable performance of the hybrid DQN-DDPG approach comes with a cost of training a model to obtain each Pareto point. However, the meta-DRL with fine-tuning approach trains only one model and to obtain a Pareto point it runs a few fine-tuning steps.

To illustrate the required training time to obtain the Pareto front, Fig. 7 illustrates the total training time versus the number of Pareto points. It is evident that the total training time of the meta-based solutions is significantly less than that of the hybrid DQN-DDPG approach, particularly for large number of Pareto points. Nonetheless, the meta-DRL with fine-tuning approach achieves a Pareto front close to that of the hybrid DQN-DDPG approach, albeit having much less total training time.

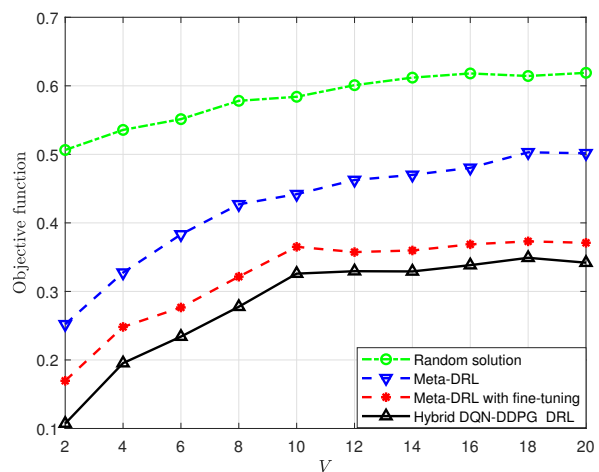


Fig. 8. Objective function in (16) versus the number of vehicles with $V = 10$ vehicles, $F = 4$ processes, $|\mathcal{R}_i| = 2$, and $\zeta = 0.5$ for the hybrid DQN-DDPG and meta-DRL with fine-tuning.

To illustrate the effectiveness of the proposed framework and solution approaches versus the number of vehicles V ,

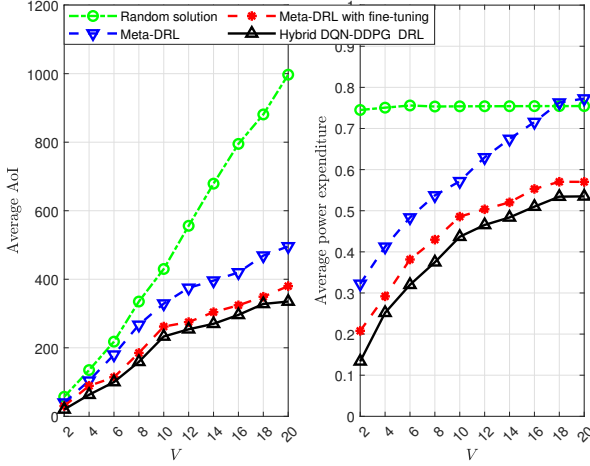


Fig. 9. Average AoI and power expenditure versus the number of vehicles with $V = 10$ vehicles, $F = 4$ processes and $|\mathcal{R}_i| = 2$, and $\zeta = 0.5$ for the hybrid DQN-DDPG and meta-DRL with fine-tuning.

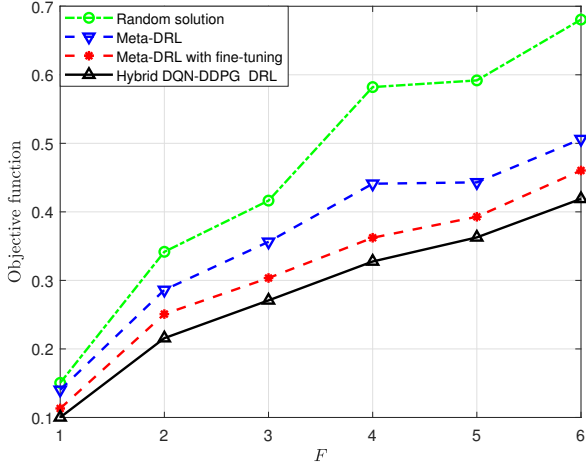


Fig. 10. Objective function in (16) versus the total number of processes F with number of process of interest per vehicle $|\mathcal{R}_i| = \lceil \frac{F}{2} \rceil$, $V = 10$ vehicles, and $\zeta = 0.5$ for the hybrid DQN-DDPG and meta-DRL with fine-tuning.

Fig. 8 and Fig. 9 illustrate the objective function in (16) and the corresponding objectives over a range of the number of vehicles, respectively. It can be seen that the proposed framework with the hybrid DQN-DDPG DRL minimizes both the AoI and power consumption, while the AoI in the random solution increases rapidly as the number of vehicles increases. It can also noticed that the meta-DRL solution minimizes the AoI and power consumption even though it was trained using randomly selected objective-preference weights. The adaptation capability of the meta-DRL model can be inferred as well as the performance of the meta-DRL with fine-tuning is close to that of the conventional DRL.

Figures 10 and 11 illustrate the objective function in (16) and the corresponding average AoI and power consumption over a range of the number of physical process, respectively.

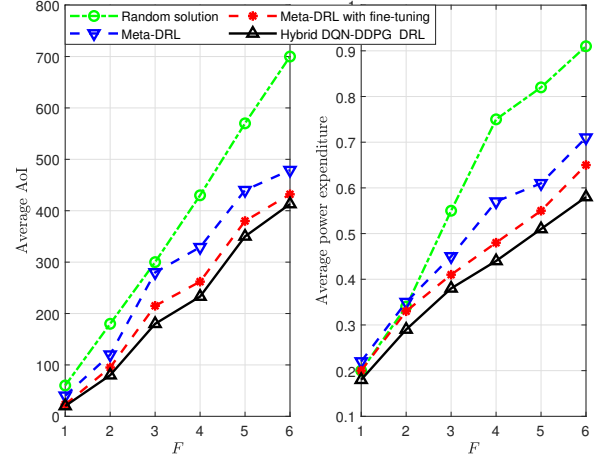


Fig. 11. Average AoI and power expenditure versus the total number of processes F with number of process of interest per vehicle $|\mathcal{R}_i| = \lceil \frac{F}{2} \rceil$, $V = 10$ vehicles, and $\zeta = 0.5$ for the hybrid DQN-DDPG and meta-DRL with fine-tuning.

It is worth mentioning that in these figures as the number of physical process increases the number of required process per vehicle is also increases (i.e., $|\mathcal{R}_i| = \lceil \frac{F}{2} \rceil$). It can be noticed that both the AoI and power consumption increase as the number of physical process increases, and the meta-DRL with fine-tuning solution provides better performance in comparison with the meta-DRL and random solutions.

Figures 12 and 13 show the performance of the solution approaches for a number of physical process over a range of the number of required process per vehicle. It can be noticed that both the AoI and power consumption increase as the number of required process per vehicle increases, and the meta-DRL with fine-tuning solution provides better performance in comparison with the meta-DRL and random solutions.

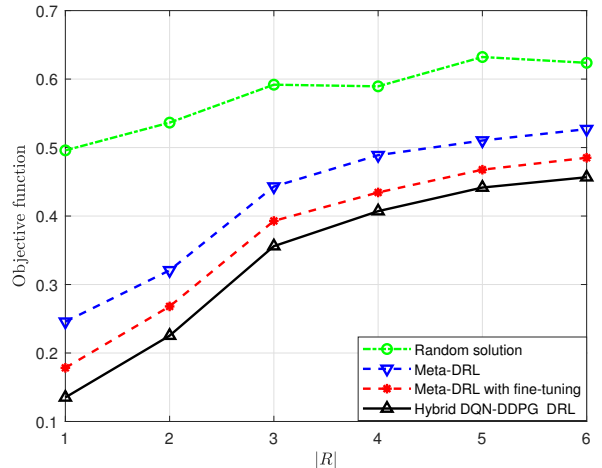


Fig. 12. Objective function in (16) versus number of process of interest per vehicle $|\mathcal{R}_i|$ with $F = 6$ processes, $V = 10$ vehicles, and $\zeta = 0.5$ for the hybrid DQN-DDPG and meta-DRL with fine-tuning.

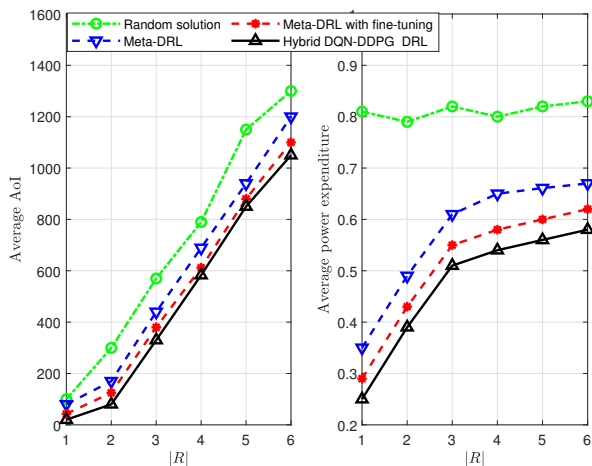


Fig. 13. Average AoI power expenditure versus number of process of interest per vehicle $|\mathcal{R}_i|$ with $F = 6$ processes, $V = 10$ vehicles, and $\zeta = 0.5$ for the hybrid DQN-DDPG and meta-DRL with fine-tuning.

To study the effect of the fine-tuning on the performance of the meta-based DRL solution, Fig. 14 illustrates the performance of the hybrid DQN-DDPG model, meta-based DRL, and meta-based DRL with fine-tuning solutions versus the number of fine-tuning steps. The hybrid DQN-DDPG model is trained with the objective-preference weight of $\zeta = 0.5$ while the meta-based DRL model is trained using randomly selected values of ζ . It can be seen that as the number of the fine-tuning steps increases the performance of meta-DRL solution with fine-tuning improves.

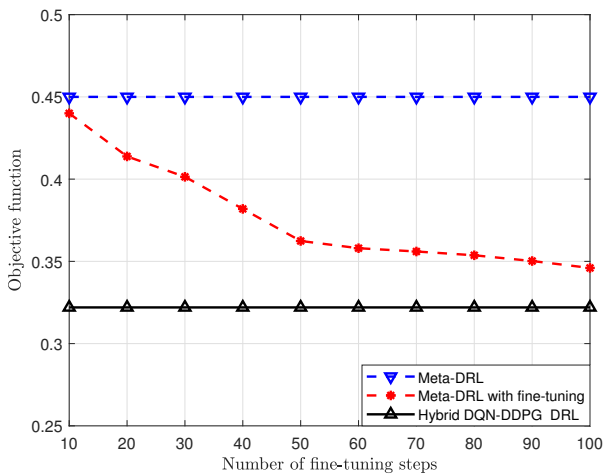


Fig. 14. Objective function in (16) versus the number of fine-tuning steps with $V = 10$ vehicles, $F = 4$ processes, $|\mathcal{R}_i| = 2$, and $\zeta = 0.5$ for the hybrid DQN-DDPG and meta-DRL with fine-tuning.

To study the effect of the vehicles' mobility and the convergence of the meta-based DRL algorithm, Fig. 15 illustrates the performance when the DRL based model is trained with vehicle speed $c_i \sim U(10, 15)$ m/s and deployed on networks with three different vehicle speed values 20, 25, and 30 m/s. It can be noticed that the algo-

rithm provides a good convergence performance and can adapt to the change in the network mobility after a few fine-tuning steps. It can be also inferred that the power required to deliver timely updates increases with the vehicles' speed, which consequently leads to a higher value of the objective function.

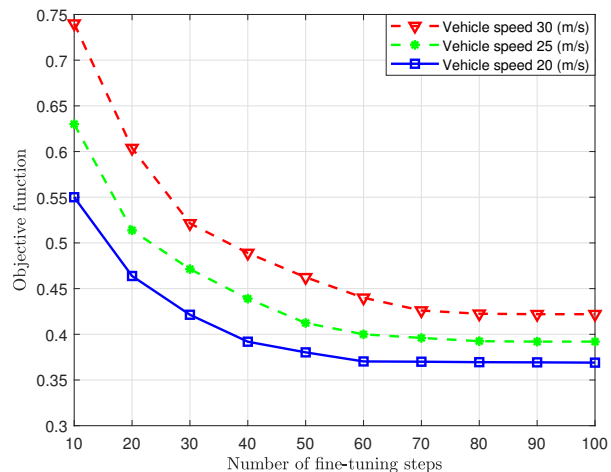


Fig. 15. Objective function in (16) versus the number of fine-tuning steps for vehicles' speeds 20, 25, and 30 m/s with $\zeta = 0.5$, $V = 10$ vehicles, $F = 4$ processes, and $|\mathcal{R}_i| = 2$.

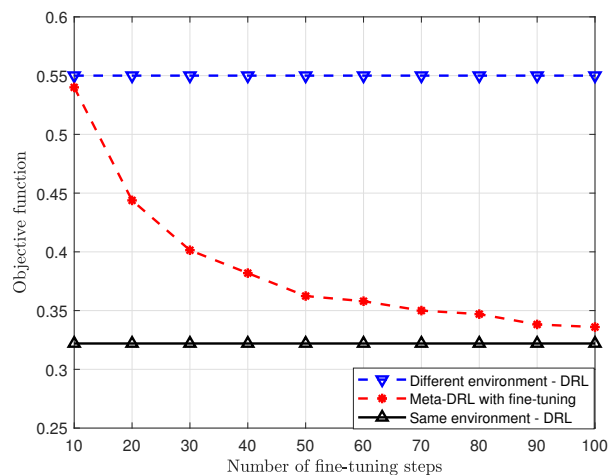


Fig. 16. Objective function in (16) versus the number of fine-tuning steps with $\zeta = 0.5$, total number of processes $F = 4$ processes and $|\mathcal{R}_i| = 2$ for two different environments (1) two lanes with $c_i \sim U(10, 15)$ m/s and (2) four lanes with $c_i \sim U(25, 35)$ m/s.

To study the generalization ability of the meta-based DRL algorithm to new physical environments, we considered two different vehicular network scenarios in Fig. 16, namely, urban environment which considers a two lanes road with velocity of the vehicle is $c_i \sim U(10, 15)$ m/s and highway environment which considers a four lanes road with velocity of the vehicle is $c_i \sim U(25, 35)$ m/s. Fig. 16 illustrates the performance of the DRL model for three different cases (1) the same-environment solution which represents the case when the DRL is trained and deployed

on the same environment (i.e., the urban environment); (2) the different-environment solution which represents the case when the DRL is trained on the urban environment and deployed on the highway environment; and (3) the meta-DRL with fine-tuning solution which represents the case when the DRL is trained on the urban environment fine-tuned and deployed on the highway environment. It can be seen that the meta-DRL model has a good generalization ability and can fast adapt to new environments via a few fine-tuning steps.

7 CONCLUSION

This paper has proposed an SIC-enabled message superposition framework to disseminate timely status updates about a set of physical processes to a set of vehicles. A multi-objective mixed integer optimization problem has been formulated to minimize both the average AoI and power consumption objectives in vehicular networks. A hybrid DQN-DDPG DRL model has been developed to solve the optimization problem. To address the tradeoff between the two objectives, a meta-based DRL algorithm is trained using a range of objective-preference weights and undergoes a few fine-tuning update steps to estimate the Pareto points of the problem. Simulation results have illustrated that the hybrid DQN-DDPG solution minimizes both the AoI and power consumption for the given objective-preference weight. Moreover, the meta-model demonstrates a rapid and excellent adaptability to estimate a high quality Pareto frontier for all problem instances, including those with either unseen objective-preference weights or the new vehicular environments. Considering DRL-based solution to handle more than two conflicting metrics in vehicular networks is considered as a future work.

REFERENCES

- [1] S. Zhang, J. Chen, F. Lyu, N. Cheng, W. Shi, and X. Shen, "Vehicular communication networks in the automated driving era," *IEEE Commun. Mag.*, vol. 56, no. 9, pp. 26–32, 2018.
- [2] Z. Li, L. Xiang, and X. Ge, "Age of information modeling and optimization for fast information dissemination in vehicular social networks," *IEEE Trans. Veh. Technol.*, vol. 71, no. 5, pp. 5445–5459, 2022.
- [3] S. Kaul, R. Yates, and M. Gruteser, "Real-time status: How often should one update," in *Proc. IEEE INFOCOM*, 2012, pp. 2731–2735.
- [4] Y. Ren, F. Liu, Z. Liu, C. Wang, and Y. Ji, "Power control in D2D-based vehicular communication networks," *IEEE Trans. Veh. Technol.*, vol. 64, no. 12, pp. 5547–5562, 2015.
- [5] X. Chen, C. Wu, T. Chen, H. Zhang, Z. Liu, Y. Zhang, and M. Bennis, "Age of information aware radio resource management in vehicular networks: A proactive deep reinforcement learning perspective," *IEEE Trans. Wirel. Commun.*, vol. 19, no. 4, pp. 2268–2281, 2020.
- [6] M. Samir, C. Assi, S. Sharafeddine, D. Ebrahimi, and A. Ghayeb, "Age of information aware trajectory planning of UAVs in intelligent transportation systems: A deep learning approach," *IEEE Trans. Veh. Technol.*, vol. 69, no. 11, pp. 12 382–12 395, 2020.
- [7] Y. Yuan, G. Zheng, K.-K. Wong, and K. B. Letaief, "Meta-reinforcement learning based resource allocation for dynamic V2X communications," *IEEE Trans. Veh. Technol.*, vol. 70, no. 9, pp. 8964–8977, 2021.
- [8] C. Liu, X. Xu, and D. Hu, "Multiobjective reinforcement learning: A comprehensive overview," *IEEE Trans. Syst. Man Cybern. Syst.*, vol. 45, no. 3, pp. 385–398, 2015.
- [9] S. Zarandi, A. Khalili, M. Rasti, and H. Tabassum, "Multi-objective energy efficient resource allocation and user association for in-band full duplex small-cells," *IEEE Trans. Green Commun. Netw.*, vol. 4, no. 4, pp. 1048–1060, 2020.
- [10] R. Hashemi, H. Beyranvand, M. R. Mili, A. Khalili, H. Tabassum, and D. W. K. Ng, "Energy efficiency maximization in the uplink Delta-OMA networks," *IEEE Trans. Veh. Technol.*, vol. 70, no. 9, pp. 9566–9571, 2021.
- [11] I. Y. Kim and O. De Weck, "Adaptive weighted sum method for multiobjective optimization: A new method for Pareto front generation," *Struct. Multidiscipl. Optim.*, vol. 31, no. 2, pp. 105–116, 2006.
- [12] R. T. Marler and J. S. Arora, "Survey of multi-objective optimization methods for engineering," *Structural and multidisciplinary optimization*, vol. 26, no. 6, pp. 369–395, 2004.
- [13] O. B. Augusto, F. Bennis, and S. Caro, "A new method for decision making in multi-objective optimization problems," *Pesquisa Operacional*, vol. 32, pp. 331–369, 2012.
- [14] C. Finn, P. Abbeel, and S. Levine, "Model-agnostic meta-learning for fast adaptation of deep networks," in *Proc. International conference on machine learning*. PMLR, 2017, pp. 1126–1135.
- [15] Z. Zhang, Z. Wu, H. Zhang, and J. Wang, "Meta-learning-based deep reinforcement learning for multiobjective optimization problems," *IEEE Trans. Neural Netw. Learn. Syst.*, pp. 1–14, 2022.
- [16] X. Chen, A. Ghadirzadeh, M. Björkman, and P. Jensfelt, "Meta-learning for multi-objective reinforcement learning," in *Proc. IEEE International Conference on Intelligent Robots and Systems (IROS)*. IEEE, 2019, pp. 977–983.
- [17] Y. Ni, L. Cai, and Y. Bo, "Vehicular beacon broadcast scheduling based on age of information (AoI)," *China Commun.*, vol. 15, no. 7, pp. 67–76, 2018.
- [18] M. K. Abdel-Aziz, S. Samarakoon, C.-F. Liu, M. Bennis, and W. Saad, "Optimized age of information tail for ultra-reliable low-latency communications in vehicular networks," *IEEE Trans. Commun.*, vol. 68, no. 3, pp. 1911–1924, 2020.
- [19] M. Chen, Y. Xiao, Q. Li, and K.-c. Chen, "Minimizing age-of-information for fog computing-supported vehicular networks with deep Q-learning," in *Proc. IEEE International Conference on Communications (ICC)*, 2020, pp. 1–6.
- [20] L. Yang, J. Chen, Q. Ni, J. Shi, and X. Xue, "NOMA-enabled cooperative unicast-multicast: Design and outage analysis," *IEEE Trans. Wirel. Commun.*, vol. 16, no. 12, pp. 7870–7889, 2017.
- [21] J. Wang, H. Xu, B. Zhu, L. Fan, and A. Zhou, "Hybrid beamforming design for mmWave joint unicast and multicast transmission," *IEEE Commun. Lett.*, vol. 22, no. 10, pp. 2012–2015, 2018.
- [22] W. Hao, G. Sun, F. Zhou, D. Mi, J. Shi, P. Xiao, and V. C. M. Leung, "Energy-efficient hybrid precoding design for integrated multicast-unicast millimeter wave communications with SWIPT," *IEEE Trans. Veh. Technol.*, vol. 68, no. 11, pp. 10956–10 968, 2019.
- [23] M. Sadeghi, E. Björnson, E. G. Larsson, C. Yuen, and T. Marzetta, "Joint unicast and multi-group multicast transmission in massive MIMO systems," *IEEE Trans. Wirel. Commun.*, vol. 17, no. 10, pp. 6375–6388, 2018.
- [24] Y. Chen, H. Tang, and J. Wang, "Optimizing age of information in multicast unilateral networks," in *Proc. IEEE International Symposium on Broadband Multimedia Systems and Broadcasting (BMSB)*, 2020, pp. 1–4.
- [25] X. Yuan, J. Chen, N. Zhang, J. Ni, F. R. Yu, and V. C. M. Leung, "Digital twin-driven vehicular task offloading and IRS configuration in the internet of vehicles," *IEEE Trans. Intell. Transp. Syst.*, vol. 23, no. 12, pp. 24 290–24 304, 2022.
- [26] X. Yuan, J. Chen, N. Zhang, Q. Ye, C. Li, C. Zhu, and X. S. Shen, "Low-cost federated broad learning for privacy-preserved knowledge sharing in the RIS-aided internet of vehicles," *Engineering*, 2023.
- [27] J. Li, Y. Zhou, and H. Chen, "Age of information for multicast transmission with fixed and random deadlines in IoT systems," *IEEE Internet Things J.*, vol. 7, no. 9, pp. 8178–8191, 2020.
- [28] S. Nath, J. Wu, and J. Yang, "Optimum energy efficiency and age-of-information tradeoff in multicast scheduling," in *Proc. IEEE International Conference on Communications (ICC)*, 2018, pp. 1–6.
- [29] M. Xie, J. Gong, X. Jia, and X. Ma, "Age and energy tradeoff for multicast networks with short packet transmissions," *IEEE Trans. Commun.*, vol. 69, no. 9, pp. 6106–6119, 2021.
- [30] M. Zhou, J. Li, J. Yuan, M. Xie, W. Tan, R. Yin, and L. Yang, "An architecture for AoI and cache hybrid multicast/unicast/D2D with cell-free massive MIMO systems," *IEEE Access*, vol. 11, pp. 43 080–43 088, 2023.
- [31] A. Al-Habob, H. Tabassum, and O. Waqar, "Dynamic unicast-multicast scheduling for age-optimal information dissemination

- in vehicular networks," in *Proc. IEEE Globecom Workshops (GC Wkshps)*, 2022, pp. 1218–1223.
- [32] W. Yuan, Z. Wei, S. Li, J. Yuan, and D. W. K. Ng, "Integrated sensing and communication-assisted orthogonal time frequency space transmission for vehicular networks," *IEEE J. Sel. Top. Signal Process.*, vol. 15, no. 6, pp. 1515–1528, 2021.
- [33] Z. Yang, J. A. Hussein, P. Xu, Z. Ding, and Y. Wu, "Power allocation study for non-orthogonal multiple access networks with multicast-unicast transmission," *IEEE Trans. Wirel. Commun.*, vol. 17, no. 6, pp. 3588–3599, 2018.
- [34] M. Sadeghi and C. Yuen, "Multi-cell multi-group massive MIMO multicasting: An asymptotic analysis," in *Proc. IEEE Global Communications Conference (GLOBECOM)*, 2015, pp. 1–6.
- [35] M. Sadeghi, E. Björnson, E. G. Larsson, C. Yuen, and T. L. Marzetta, "Max-min fair transmit precoding for multi-group multicasting in massive MIMO," *IEEE Trans. Wirel. Commun.*, vol. 17, no. 2, pp. 1358–1373, 2018.
- [36] C. She, C. Sun, Z. Gu, Y. Li, C. Yang, H. V. Poor, and B. Vucetic, "A tutorial on ultrareliable and low-latency communications in 6G: Integrating domain knowledge into deep learning," *Proc. IEEE*, vol. 109, no. 3, pp. 204–246, 2021.
- [37] X. Ma, Y. Yu, X. Li, Y. Qi, and Z. Zhu, "A survey of weight vector adjustment methods for decomposition-based multiobjective evolutionary algorithms," *IEEE Trans. Evol. Comput.*, vol. 24, no. 4, pp. 634–649, 2020.
- [38] R. S. Sutton and A. G. Barto, *Reinforcement Learning: An Introduction*. MIT Press, 2018.
- [39] V. Mnih *et al.*, "Human-level control through deep reinforcement learning," *Nature*, vol. 518, no. 7540, pp. 529–533, Feb. 2015.
- [40] T. P. Lillicrap *et al.*, "Continuous control with deep reinforcement learning," *arXiv preprint arXiv:1509.02971*, 2015.
- [41] D. P. Kingma and J. Ba, "Adam: A method for stochastic optimization," in *Proc. Int. Conf. Learn. Representations*, 2015.
- [42] P. Sunehag, G. Lever, A. Gruslys, W. M. Czarnecki, V. Zambaldi, M. Jaderberg, M. Lanctot, N. Sonnerat, J. Z. Leibo, K. Tuyls *et al.*, "Value-decomposition networks for cooperative multi-agent learning," *arXiv preprint arXiv:1706.05296*, 2017.
- [43] —, "Value-decomposition networks for cooperative multi-agent learning based on team reward," in *Proceedings of the 17th International Conference on Autonomous Agents and MultiAgent Systems*, 2018, pp. 2085–2087.
- [44] H. Kim, S. Kim, D. Lee, and I. Jang, "Avoiding collaborative paradox in multi-agent reinforcement learning," *ETRI Journal*, vol. 43, no. 6, pp. 1004–1012, 2021.
- [45] K. Ji, J. Yang, and Y. Liang, "Theoretical convergence of multi-step model-agnostic meta-learning," *J. Mach. Learn. Res.*, vol. 23, pp. 29–70, 2022.
- [46] A. P. Guerreiro, C. M. Fonseca, and L. Paquete, "The hypervolume indicator: Problems and algorithms," *arXiv preprint arXiv:2005.00515*, 2020.



Ahmed A. Al-habob (S'15-M'22) received the BSc degree in telecommunications and computer engineering from Taiz University, Yemen, in 2009. He received the MSc degree in telecommunications from the Electrical Engineering Department, King Fahd University of Petroleum and Minerals (KFUPM), Saudi Arabia, in 2016. He received the Ph.D. degree in Electrical Engineering from the Faculty of Engineering and Applied Science, Memorial University, St. John's, NL, Canada, in 2022. He was a Postdoctoral Visitor at Lassonde School of Engineering, York University, Toronto, ON, Canada. He is currently a Postdoctoral Fellow at Memorial University of Newfoundland, NL, Canada. His research interest includes wireless communications and networking.

tor at Lassonde School of Engineering, York University, Toronto, ON, Canada. He is currently a Postdoctoral Fellow at Memorial University of Newfoundland, NL, Canada. His research interest includes wireless communications and networking.



Hina Tabassum (Senior Member, IEEE) received the Ph.D. degree from the King Abdullah University of Science and Technology (KAUST). She is currently an Associate Professor with the Lassonde School of Engineering, York University, Canada, where she joined as an Assistant Professor, in 2018. She is also appointed as the York Research Chair of 5G/6G-enabled mobility and sensing applications (2023 - 2028). She was a postdoctoral research associate at University of Manitoba, Canada. She has published over

100 refereed papers in well-reputed IEEE journals, magazines, and conferences. She received the Lassonde Innovation Early-Career Researcher Award in 2023 and the N2Women: Rising Stars in Computer Networking and Communications in 2022. She was listed in the Stanford's list of the World's Top 2% Researchers in 2021, 2022, and 2023. She is the Founding Chair of the Special Interest Group on THz communications in IEEE Communications Society (ComSoc)-Radio Communications Committee (RCC). She served as an Associate Editor for IEEE Communications Letters (2019–2023), IEEE Open Journal of the Communications Society (OJCOMS) (2019–2023), and IEEE Transactions on Green Communications and Networking (TGCN) (2020–2023). Currently, she is also serving as an Area Editor for IEEE OJCOMS and an Associate Editor for IEEE Transactions on Communications, IEEE Transactions on Wireless Communications, and IEEE Communications Surveys and Tutorials. She has been recognized as an Exemplary Editor by the IEEE Communications Letters (2020), IEEE OJCOMS (2023), and IEEE TGCN (2023). Her research interests include multi-band optical, mm-wave, and THz networks and cutting-edge machine learning solutions for next generation wireless communication and sensing networks.



Omer Waqar received the B.Sc. degree in electrical engineering from the University of Engineering and Technology (UET), Lahore, Pakistan, in 2007 and the Ph.D. degree in electrical and electronic engineering from the University of Leeds, Leeds, U.K., in November 2011. From January 2012 to July 2013, he was a Research Fellow with the Center for Communications Systems Research and 5G Innovation Center (5GIC), University of Surrey, Guildford, U.K. He worked as an Assistant Professor in

UET, Lahore, Pakistan from August 2013 to June 2018. He worked as a researcher in the department of Electrical and Computer Engineering, University of Toronto, Canada from July 2018 to June 2019. He worked as an Assistant Professor in the department of Engineering, Thompson Rivers University (TRU), British Columbia (BC), Canada from August 2019 to July 2023. Since August 2023, he has been working as an Assistant Professor in the School of Computing, University of the Fraser Valley, BC, Canada and holds an adjunct faculty position at York university, Ontario, Canada. He has authored or co-authored 35+ peer-reviewed articles including top-tier journals such as IEEE Transactions on Vehicular Technology. He has secured over \$200K in research grants from the Tri-Council agency i.e., NSERC Discovery grant and NSERC Alliance grants. Currently, he is serving as an Associate Editor for the IEEE Open Journal of the Communications Society and IEEE Canadian Journal of Electrical and Computer Engineering. His current research interests include, intelligent reflecting surface aided communication systems, Deep-Learning for next generation communication networks, wireless sensing and resource allocation of wireless networks for several distributed machine learning paradigms.